Soil & Tillage Research 255 (2026) 106804

Contents lists available at ScienceDirect

Soil & Tillage Research

journal homepage: www.elsevier.com/locate/still

Surface albedo and thermal radiation dynamics under conservation and conventional agriculture in subhumid Zimbabwe

Souleymane Diop[a,b,c,d,*], Rémi Cardinael[c,d,e], Ronny Lauerwald[a], Morgan Ferlicoq[b], Christian Thierfelder[f], Regis Chikowo[e,f], Marc Corbeels[d,g], François Affholder[d,h,i], Frédéric Baudron[d], Eric Ceschia[b]

[a] Université Paris-Saclay, INRAE, AgroParisTech, UMR EcoSys, Palaiseau 91120, France
[b] CESBIO–Univ. Toulouse III/CNRS/CNES/IRD/INRA, 18 avenue Edouard Belin, Toulouse Cedex 9 31401, France
[c] CIRAD, UPR AIDA, Harare, Zimbabwe
[d] AIDA, Univ. Montpellier, CIRAD, Montpellier, France
[e] Department of Plant Production Sciences and Technologies, University of Zimbabwe, Harare, Zimbabwe
[f] International Maize and Wheat Improvement Center (CIMMYT), P.O. Box MP 163, Mount Pleasant, Harare, Zimbabwe
[g] IITA, International Institute of Tropical Agriculture, PO Box 30772, Nairobi 00100, Kenya
[h] CIRAD, UPR AIDA, Maputo, Mozambique
[i] Universidade Eduardo Mondlane, Faculdade de Agronomia e Engenharia, France

ARTICLE INFO

Keywords:
Sub-Saharan Africa
Climate change mitigation
Biogeophysical effects
No-tillage
Mulch

ABSTRACT

While conservation agriculture (CA) has been widely evaluated for its biogeochemical effects (e.g soil organic carbon sequestration and greenhouse gas emissions) for climate mitigation, its biogeophysical impacts related to changes in surface albedo remain understudied. This study assessed the biogeophysical effects of CA cropping systems with maize (*Zea mays* L.) in Zimbabwe. Measurements were conducted continuously over two cropping years at two long-term experiments with contrasting soil characteristics, on an abruptic Lixisol and on a xanthic Ferralsol. The dynamics of surface albedo, longwave radiation, leaf area index, soil moisture and temperature were monitored under three different treatments: conventional tillage (CT, tilled to ~15 cm), no-tillage (NT) and no-tillage with mulch (NTM, 2.5 t DM ha^{-1}). Our results revealed that, on the Ferralsol, NT and NTM significantly ($p < 0.05$) increased mean annual albedo (0.17) relative to CT (0.16), resulting in a negative instantaneous radiative forcing (iRF) and indicating a net cooling effect. iRF was stronger in 2021/22 (NT: -0.83 ± 0.17 W m^{-2}; NTM: -1.43 ± 0.7 W m^{-2}) than in ^{2}022/23 (NT: -0.43 ± 0.09 W m^{-2}; NTM: -1.03 ± 0.21 W m^{-2}). Conversely, on the Lixisol, while NT increased surface albedo (0.27 vs. CT: 0.24), NTM significantly reduced albedo (0.23), causing positive iRF (warming). iRF was -3.34 ± 0.69 W m^{-2} and -2.78 ± 0.77 W m^{-2} for NT in the first and second cropping year, respectively, and increased from 1.14 ± 0.21 W $^{-2}$ (2021/22) to 2.77 ± 0.41 W m^{-2} (2022/23) under NTM. Overall, our results suggest that the soil background albedo is an important site characteristic that needs to be considered and demonstrates the importance of considering biogeophysical effects when promoting practices of CA for climate change mitigation.

1. Introduction

The climate impact of cropland management is usually assessed in terms of biogeochemical effects such as soil organic carbon (SOC) sequestration (Beillouin et al., 2023) or greenhouse gas emissions (Fuentes-Ponce et al., 2022). However, cropland management also affects local heat budgets through changes in surface albedo and thus the fraction of solar radiation that is absorbed and transformed into heat energy and further through changes in the partitioning of the generated heat energy between soil heat fluxes, latent and sensible heat fluxes, and infrared radiation (Davin and de Noblet-Ducoudré, 2010; Hirsch et al., 2017; Lobell et al., 2006). Recent studies have shown that these biogeophysical effects play nonnegligible roles in the overall climate impact of land use and land management practices (Luyssaert et al., 2014), as they can substantially add to or offset positive biogeochemical effects (Betts, 2000; Kaye and Quemada, 2017; Pique et al., 2023). In croplands,

* Corresponding author at: Université Paris-Saclay, INRAE, AgroParisTech, UMR EcoSys, Palaiseau 91120, France.
E-mail address: souleymanediop@myyahoo.com (S. Diop).

https://doi.org/10.1016/j.still.2025.106804
Received 9 February 2025; Received in revised form 7 August 2025; Accepted 9 August 2025
Available online 13 August 2025
0167-1987/© 2025 The Author(s). Published by Elsevier B.V. This is an open access article under the CC BY license (http://creativecommons.org/licenses/by/4.0/).

the surface albedo may vary due to various factors, such as crop species, sowing density, crop phenological stage, soil type, topsoil organic matter content, surface roughness, soil moisture and soil coverage by mulch (Cai et al., 2016; Cierniewski et al., 2018, 2013; Matthias et al., 2000; Oguntunde et al., 2006). Changes in the surface albedo of croplands may lead to cooling or warming effects at local and global scales (Akbari et al., 2009; Betts, 2000; Sieber et al., 2022).

Conservation agriculture (CA), which covers a range of cropping practices based on minimum soil disturbance, permanent soil cover with crop residues or cover crops, and crop diversification, has been widely promoted for its positive impact on SOC sequestration, although this effect is often limited in magnitude (Corbeels et al., 2020; Franzluebbers, 2010; Powlson et al., 2016). CA practices can, however, also have strong biogeophysical effects. For example, Horton et al. (1996) reported that retaining crop residues in no-tillage systems increases the surface albedo on dark soils during bare fallow periods. Davin et al. (2014) proposed that no-tillage practices lead to local cooling of European croplands in summer due to increased albedo, outweighing reduced evaporation. Hirsch et al. (2018) modelled the biogeophysical effects of conservation agriculture, which indicated local cooling in midlatitude regions but potential warming in tropical areas. Similarly, Thierfelder and Wall (2009) found that conservation agriculture techniques improve soil infiltration and water retention in Zambia and Zimbabwe, contributing to changes in surface energy balance. Vogel (1994) also observed that tillage practices influence topsoil temperature, further highlighting the thermal and physical soil impacts of different tillage approaches. Finally, Lobell et al. (2006) reported that, globally, no-tillage systems adopted for croplands cause cooling by approximately 0.2 °C, which is comparable to their biogeochemical cooling effect.

The climatic effects of CA were evaluated mostly through the “radiative forcing” (RF) concept. RF is a metric that is used to quantify the changes in the Earth’s energy balance (radiation received and emitted by the Earth) that are induced by natural and anthropogenic drivers. Changes in RF may be a result of increasing atmospheric CO_2 concentrations that absorb and re-emit downwards more of the longwave radiation that is emitted by the surface of Earth (Betts, 2000). These changes can also result from a change in the albedo of the atmosphere (cloud cover) or of the surface (Forster et al., 2007). The effects of changes in surface albedo on climate can be quantified via RF metrics (Betts, 2000; Bright and Lund, 2021; Carrer et al., 2018; Schwaiger and Bird, 2010). However, most changes in surface albedo result in changes in energy partitioning (e.g., latent and sensible heat fluxes) and therefore in atmospheric “adjustments” that moderate the instantaneous shortwave radiative forcing (iRF) from albedo changes (Bright and Lund, 2021). Longwave radiation is also an important component of the surface energy budget (Breil et al., 2023; Bright et al., 2017; Liao et al., 2020). The net effects of changes in energy partitioning and iRF are the so-called “effective radiative forcing” (ERF), which is a better indicator of the effective impact of climate change. Recent model simulations have shown that atmospheric adjustments can either offset albedo change-driven iRF or reinforce it further (Andrews et al., 2017; Bellouin et al., 2020; Forster et al., 2016; Smith et al., 2020). Therefore, assessing the effects of cropland management on both the surface albedo and the infrared radiation emitted by the surface not only helps researchers understand the interactions between the energy flux exchanges between soil, plants and the atmosphere but also their potential interactions with greenhouse gases in the atmosphere (Aydinalp and Cresser, 2008).

In our study, we assess no-tillage and residue retention impacts on surface energy fluxes in Sub-Saharan Africa—a region where such practices have never been evaluated for their effects on albedo and longwave radiation for two soil types (an abruptic Lixisol and a xanthic Ferralsol). This study provides novel insights into how conservation agriculture practices influence albedo, soil moisture, thermal dynamics, and crop development, thereby contributing to a better understanding of the energy budget in tropical agroecosystems.

For this, we examined the effects of no-tillage and crop residue retention (two of the principles of CA) versus conventional tillage at two experimental sites with contrasting soil properties in subhumid Zimbabwe, both with maize monocultures. We evaluated the impacts of these two land management practices on the surface albedo and outgoing longwave radiation and surface temperature dynamics on a daily basis, as well as their interactions with soil type, topsoil moisture and temperature, and crop growth. We quantified also instantaneous radiative forcing (iRF) on a daily basis. Our main hypotheses are that CA has distinct effects on surface albedo dynamics and instantaneous radiative forcing as well as on longwave radiation, depending upon 1) the presence or absence of soil tillage and crop residues on the soil surface, 2) the soil type, and 3) the controlling effects of crop growth and soil moisture dynamics.

2. Materials and methods

2.1. Experimental sites

The study was carried out at two experimental sites in Zimbabwe, established in 2013 by the International Maize and Wheat Improvement Center (CIMMYT): the Domboshawa Training Center (DTC) site in the district of Goromonzi (17°36’23.3"S; 31°08’26.8’’E), located approximately 30 km north of Harare, and the University of Zimbabwe Farm (UZF) site in the district of Mazowe (17°43’15.1"S; 31°01’15.8"E), located approximately 10 km north of Harare and approximately 20 km from the DTC site. The experimental sites are characterized by two different soil classes: an abruptic Lixisol (light-coloured red sandy soil, FAO classification, 1997) at DTC and a xanthic Ferralsol (dark-coloured yellowish-brown clayey, FAO classification, 1997) at UZF. The soil at the DTC has a light texture in the top 0–20 cm layer (sandy loam with 15 % clay), with an abrupt textural change to sandy clay loam with 30 % clay in the 20–40 cm layer (Shumba et al., 2023). The soil texture at UZF is sandy-clay-loam with 34 % clay in the first 20 cm (Shumba et al., 2023). The sites both have a subtropical climate with annual minimum and maximum mean temperatures of 12 °C and 25 °C, respectively, and a rainy season from November to April (Mapanda et al., 2010; Shumba et al., 2023) (Fig. 1). In our study, we conducted field measurements during two cropping years from October 2021 to October 2023. At the DTC, the cumulative rainfall amounts during the first (2021/22) and second (2022/23) cropping years were 1219 mm and 1132 mm, respectively. At UZF, the total rainfall amounts were 907 mm and 941 mm during the first and second cropping years, respectively.

2.2. Experimental treatments

An identical experimental design was set up at both sites, and the treatments were the same in every season since the beginning of the experiment. The dimensions of the experimental plots were 12 × 6 m, and the main crop was maize (*Zea mays* L.). For our study, we considered three of the eight treatments that were established at the sites (Mhlanga et al., 2022): conventional tillage (CT), no-tillage (NT) and no-tillage with mulch (NTM) with continuous maize cropping (). The maize crop was sown with a spacing of 25 cm within rows and 90 cm between rows to achieve a plant density of 44,444 plants ha^{-1}. Two or three seeds were sown per planting hole, and the crop was thinned to one plant per pit after emergence. In the CT treatment, tillage was performed at 15 cm with a hand hoe at both sites, and all the maize residues were removed after harvest. In the NT and NTM treatments, the soil was not tilled, and the maize was sown in planting basins dug with a hand hoe at approximately 15 cm depth at UZF, whereas at DTC, the seeds were placed in riplines made with an animal-drawn ripper (Magoye ripper). Compound fertilizers (nitrogen (N), phosphorus (P) and potassium (K)) were applied to the maize rows at sowing at application rates of 11.6 kg N ha^{-1}, 10.6 kg P ha^{-1} and 9.6 kg K ha^{-1}, respectively. The first and second

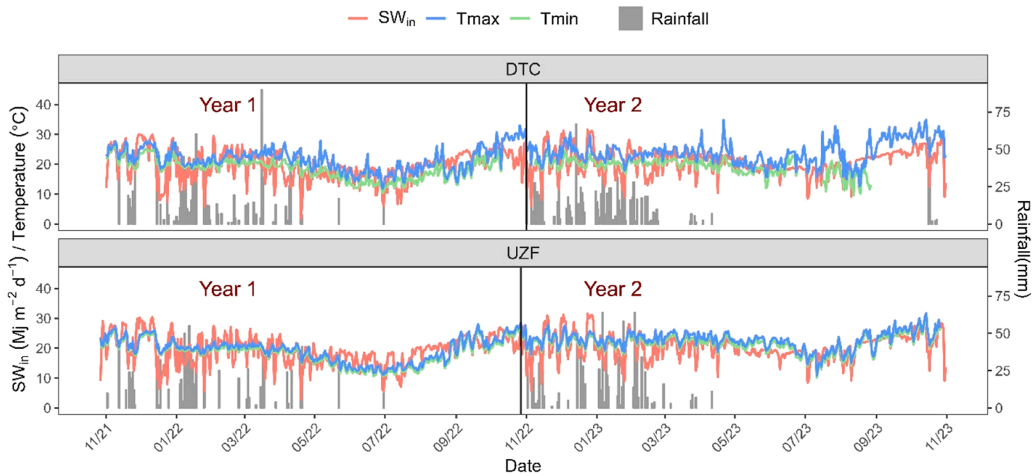

Fig. 1. Daily temperatures, shortwave incoming solar radiation and rainfall over two cropping years at the DTC and UZF sites.

top dressings were applied four and eight weeks after sowing, respectively, with 23 kg N ha^{-1} each in the form of ammonium nitrate (Shumba et al., 2023).

In the NTM treatment, 2.5 t DM ha^{-1} of maize residue from the previous cropping season was placed on the soil surface approximately two weeks before sowing the maize. After the maize harvest, farmers practising CA in Zimbabwe frequently store their crop residues during the dry season to avoid their consumption by cattle that freely graze in fields during that period. Mulch is thus applied shortly before sowing in the following season, when the cattle are moved to grazing areas away from cultivated land. In that case, the soil is bare during the dry season, even under CA. However, some farmers in Zimbabwe have fences around their fields to prevent cattle grazing and prefer to leave the residues on the soil after harvest, as do most CA practitioners globally, and the soil is never bare. To investigate the impacts of these two management options on the albedo, outgoing longwave radiation and surface temperature dynamics, we varied the setup of the NTM between the first and second cropping years. In the first cropping year, the soil was not covered in the dry season, whereas in the second cropping year, crop residues were directly applied to the soil after harvest and remained there during both the dry and growing seasons. Based on the image processing of pictures taken approximately 1.5 m above the plots four weeks after mulch application, we estimated that the mulch covered 45 % of the soil. Additionally, the kinetic decomposition of the mulch was assessed within 0.25-m^2 quadrats that were sampled on six different dates. The results revealed that 70 % and 36 % of the mulch at UZF and DTC, respectively, decomposed within three months after application (Figure S3).

2.3. Field measurements

2.3.1. Shortwave and longwave radiation sensors

The sites were equipped with three 4-component net radiometers (NR01, Hukseflux Thermal Sensors, Delft, Netherlands) to monitor incoming (in) and outgoing (out) shortwave (SW) and longwave (LW) radiation (SW_{in}, SW_{out}, LW_{in}, LW_{out}, respectively) for each treatment. This type of radiometer is commonly used for surface albedo monitoring (Sieber et al., 2019). It consists of a pair of pyranometers and a pair of pyrgeometers, with one pair facing upwards and the other facing downwards (Diop, 2023).

The pyranometers measure SW solar radiation in the wavelength spectrum from 0.3 to 2.8 µm, which encompasses the visible and near-infrared spectra. The surface albedo (α) is derived from the two opposite directions of the pyranometer measurements and is calculated with the following equation:

$$\alpha = \frac{SW_{out}}{SW_{in}} \tag{1}$$

where α is the surface albedo, SW_{out} (W m^{-2}) is the amount of solar radiation that is reflected by the Earth's surface and SW_{in} (W m^{-2}) is the global incoming solar radiation.

In our study, the surface albedo was measured continuously at both experimental sites during the growing season from November to April and during the dry season corresponding to the bare fallow period from May to October.

The pyrgeometers are thermal sensors that measure the incoming and outgoing longwave radiation (LW_{in}, LW_{out}, respectively) expressed in W m^{-2} in the wavelength spectrum between 4.5 and 50 µm.

The four-component net radiometers were mounted horizontally on a mast and placed 1.5 m above the ground during the bare fallow period, with a field of view (FOV) of 180° for the pyranometers and 150° for the pyrgeometers. During the growing season, the height of the instruments was adjusted each week to maintain a distance of 1.5 m above the plant canopy. The masts were placed in the middle of the plots to avoid edge effects due to the surrounding land surfaces. The energy balance studies should follow the ISO/TR 9901 guidelines. This norm recommends the height at which the sensors should be mounted to minimize the errors from shadowing effects and to maximize the signal that comes from the targeted area. For small plots, the recommended height is between 1.5 and 2 m. The challenge in this case is to ensure that the FOV of the downfacing sensors targets the area of interest (sample) as much as possible and avoids mixing with signals from the surrounding areas. A downfacing pyranometer positioned at a height *h* above the area of interest with a radius of *X sample* metres subtends an angle from the nadir expressed as follows:

$$\theta_{sample} = \tan^{-1}\left(\frac{Xsample}{h}\right) \tag{2}$$

The contribution of the area of interest to be sampled relative to the total signal measured corresponds to the sine of Θ_{sample}. In our study, the sensors were mounted 1.5 m above the target 3 m from the nearest border of the plot, meaning that the total contribution of the plot to be sampled was 89 % of the total signal. The remaining 11 % of the signal originates from the surrounding areas outside the plot, which were also cropped with maize and therefore have very similar albedo values. We thus conclude that the degree of pollution of our observed signal with contributions from outside the plot of interest is acceptable. Moreover, in our study, we are more interested in the relative changes in surface albedo between treatments (to calculate radiative forcing), specifically no-tillage vs. tillage and mulch vs. no mulch, than in absolute albedo values. As the protocols used to measure shortwave and longwave radiation are similar across treatments as well as the surrounding cover around the plots, our measurements can be considered robust.

The radiometers were connected to a CR1000 datalogger (Campbell Scientific Inc., Logan, UT, USA), which recorded data every minute. The data were then averaged at half-hourly intervals.

During the measurement campaign, we encountered technical issues with the pyranometers for a few days during the dry season between September and October, leading to a loss of albedo data at DTC. These data gaps were filled using the albedo-soil moisture relationship developed for the treatments at this site (see Table S1 in the Supplemental Materials). We conducted a validation exercise by artificially removing a subset of observed albedo data and then applying our linear gap-filling models to estimate the missing values. These estimates were then compared with the actual observed values to assess the reliability of the approach. We also encountered a technical problem when monitoring the longwave radiation at the UZF site during an extended period of the first year, which caused considerable data gaps at this site that could not be filled.

2.3.2. Weather station and soil sensors

A weather station, ATMOS 41 (Meter Group, Inc., Pullman, WA, USA), was used to monitor the air temperature, relative humidity, wind speed and direction, rainfall and vapour pressure. These data were recorded on a second datalogger (METER ZL6, Meter Group, Inc., Pullman, WA, USA). The high-frequency measurements (every minute) were averaged at half-hourly time intervals to be consistent with the radiometer measurements.

The soil temperature and soil moisture were monitored at 1, 10, and 20 cm soil depths and at 5-minute intervals with ECH2O sensors (Meter Group, Inc., Pullman, WA, USA) in each of the plots equipped with NR01 sensors. The ECH2O sensors were connected to the METER ZL6 datalogger. These sensors were installed in the middle of the plots between two maize rows, inserted horizontally in the soil (Figure S4). PVC access tubes were installed to a depth of 105 cm, and soil moisture was monitored using a neutron probe calibrated through gravimetric sampling. Calibration involved installing additional access tubes outside the plots, applying water to field capacity, and sampling at various depths until wilting point. Although the ECH2O sensors were not directly calibrated, their continuous measurements closely aligned with neutron probe data across plots, supporting the reliability of the sensor outputs.

2.3.3. Crop measurements

The plant area index (PAI) is the ratio of the total plant area (e.g., leaves, stems, and organs) per soil surface area expressed in square metres of the plant surface per square metre of the soil surface. It is a key indicator used to evaluate vegetation structure (Yan et al., 2019) and is closely related to the CO_2, water and energy fluxes at the plant stand level (Béziat, 2009; Béziat et al., 2013). In our study, we used an LAI 2200 C plant canopy analyser (LI-COR Biosciences, Lincoln, NE, USA) to obtain indirect measurements of the PAI. We monitored the PAI every two weeks during the two cropping years. A measurement consisted of one acquisition above the crop canopy and four acquisitions on the diagonal, one on the maize row, one at 25 % from the row, one in the middle of two rows and one at 75 % distance between two rows from the starting point. The measurements were repeated six times per plot at each site to better integrate the field variability in crop growth. The FV2200 software of the LAI-2200 plant canopy analyser was used to process the data and to compute the means and standard deviations of the PAI for each treatment and measurement date.

The green fractional canopy cover (GFCC) is closely related to crop growth, light interception and evapotranspiration (Irmak and Kukal, 2022). The GFCC was obtained via the Canopeo® mobile application developed at Oklahoma State University (Patrignani and Ochsner, 2015). Canopeo® is a tool that uses a simple classification of the pixels in a photograph based on the excess green ratio. The output of Canopeo® is a binary image that is composed of white pixels representing high green ratios and black pixels representing the nongreen parts of plants. It has been used in several studies to monitor the GFCC (Jàuregui et al., 2019; Liang et al., 2012), including in Zimbabwe (Namatsheve et al., 2024).

2.4. Instantaneous radiative forcing

We calculated the instantaneous radiative forcing (iRF) (i.e., radiative forcing without accounting for possible changes in the temperature of the troposphere; see the IPCC 2018 glossary) values at the top of the atmosphere (TOA) for the NT and NTM treatments compared with the CT treatment during two years at the two experimental sites by using the method of Muñoz et al. (2010) as follows:

$$iRF\triangle\alpha(i) \quad = \quad -SW_{in(i)} \times Ta(i) \times \triangle\alpha(i) \tag{3}$$

$$\text{with } Ta(i) = \frac{SW_{in}}{R_{TOA}} \tag{4}$$

where $SW_{in(i)}$ represents the daily incoming shortwave solar radiation of day i in W m^{-2}, $Ta(i)$ represents the atmospheric transmittance of day i, and R_{TOA} represents the radiation at the top of the atmosphere. Ta is calculated at the daily time step in contrast to using a mean annual constant Ta of approximately 0.85, as applied in Lenton and Vaughan (2009). The R_{TOA} is calculated as a function of latitude by using a sophisticated equation involving time according to the Fu–Liou radiative transfer model (Fu and Liou, 1993), as in Carrer et al., (2018). $\Delta\alpha$ is the daily mean surface albedo difference between a given treatment, namely, NT or NTM and a reference, which is the CT treatment in this study. The result is expressed in W m^{-2}. Positive iRF values represent a warming effect on climate, whereas negative values represent a cooling effect on climate.

2.5. Uncertainties and assumptions

Our experimental design introduces inherent uncertainties in the measurements that we quantified considering the accuracy of the sensors, the uncertainty caused by the gap-filling procedure applied to all treatments at the DTC site in 2022/23 and 2022/23 and because of the angle of view and height of the sensors measuring SW_{out}. The radiometers used for monitoring shortwave and longwave radiation have an estimated accuracy of ±10 % for both pyranometers and pyrgeometers, which propagates to uncertainties in surface albedo, instantaneous radiative forcing (iRF), and outgoing longwave radiation calculations. Similarly, the ECH2O soil moisture and temperature sensors exhibit an accuracy of ±3 % respectively ±1 %, affecting correlations between topsoil moisture and albedo dynamics. Data gaps due to technical issues such as pyranometer failures during dry seasons and extended longwave radiation monitoring failures at the DTC site were filled using empirical albedo-soil moisture relationships, introducing additional uncertainty from model extrapolation. Furthermore, the 1.5 m sensor height and 150–180° field of view measuring SW_{out} captured ~89 % of the target plot signal, but the remaining 11 % from surrounding areas with similar albedo values may bias treatment-specific results. Collectively, these instrumental and methodological uncertainties could bias the reported iRF values by up to ±15–20 %.

2.6. Statistical analyses

The statistical analyses were conducted using R software (Core Team 2023). First, we checked whether the data had a normal distribution by using the Shapiro-Wilk test and visualized it with quantile—quantile plots. Differences in the seasonal variations in the surface albedo were analysed via one-way ANOVA based on linear mixed models using the *ggpubr* package (Kassambara, 2023) with treatments, sites and seasons as fixed effects, and day nested within seasons as random effects to account for temporal auto-correlation. The fitted model was chosen based on the lowest Bayesian information criterion (BIC). The statistical significance of the differences was tested via Tukey's HSD test at a p value < 0.05.

3. Results

3.1. Effects of treatments and soil type on the surface albedo

The daily surface albedo dynamics across the different treatments, namely, conventional tillage (CT), no-tillage (NT), and no-tillage with mulch (NTM), varied at the two experimental sites, UZF and DTC, during the two cropping years (Fig. 2 A, C). Globally, the surface albedo is greater at DTC than at UZF. Before sowing, high albedo values were observed at both sites. During the period from soil preparation to maize emergence, the CT treatment had a lower albedo than did the NT and NTM treatments at both sites. This difference was attributed to tillage in

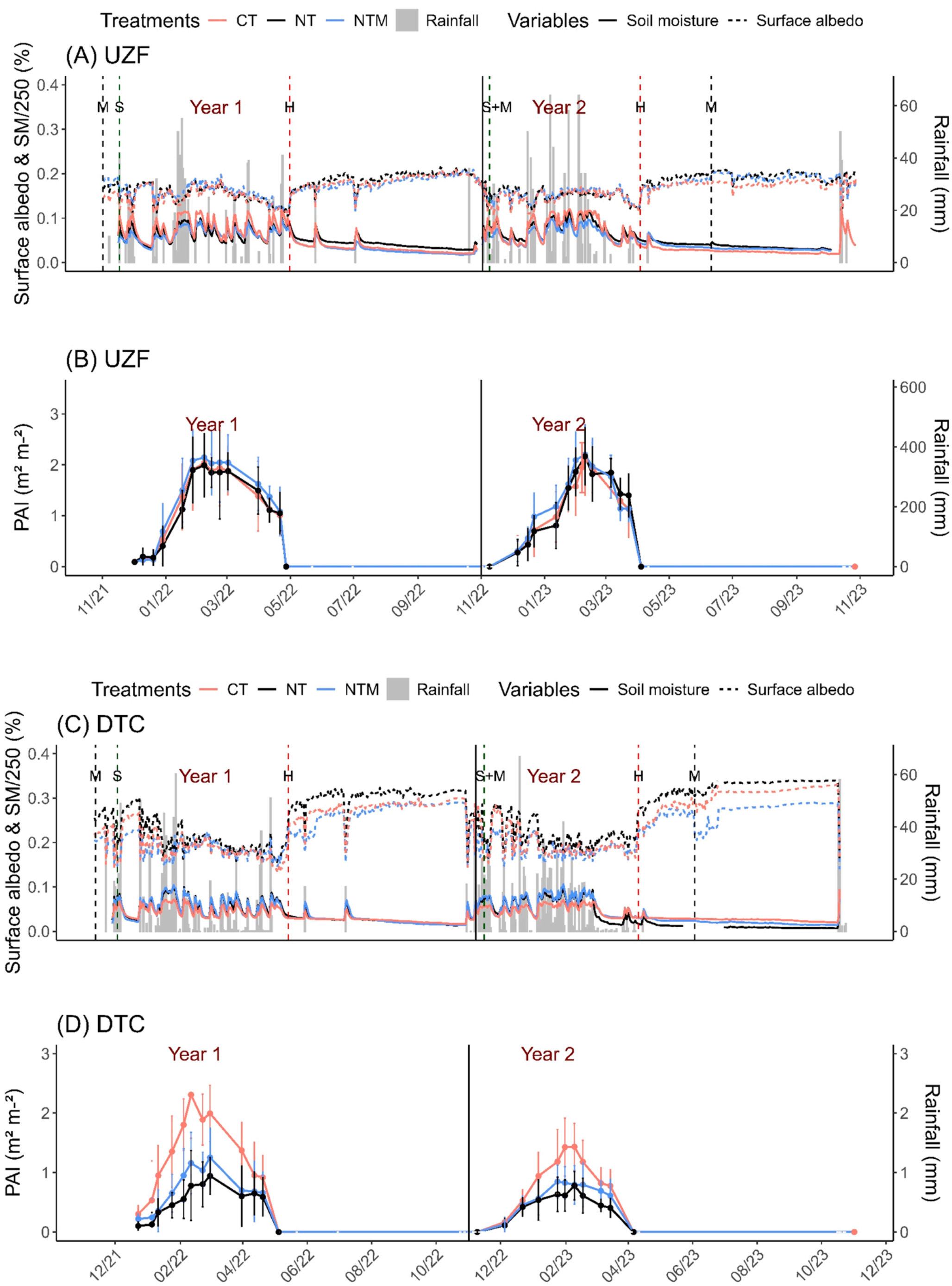

Fig. 2. (A, C) The dynamics of the top (1 cm depth) soil moisture (SM) divided by 250 to fit at the same y-Axis as the surface albedo (dashed lines) and the surface albedo (solid lines) at UZF (Ferralsol, dark-coloured) and DTC (Lixisol, light-coloured),) for three treatments: conventional tillage (CT, salmon); no-tillage (NT, black); and no-tillage with mulch (NTM, blue) during the 1st (2021/22) and 2nd (2022/23) cropping years in Zimbabwe. (B, D) Plant area index (PAI) dynamics at UZF and DTC, respectively. The error bars represent the standard deviations (N = 6). The light grey bars represent daily rainfall. The vertical green dashed lines represent the maize sowing dates, the red dashed lines represent the harvest dates, and the black dashed lines represent the application of mulch. S: Sowing, H: Harvest, and M: Mulching. The solid vertical dark lines represent the end of the first cropping year and the beginning of the second cropping year. Tillage and mulching in the first cropping year were performed before the start of the measurements. Tillage and the 1st mulch application during the second cropping year were performed at maize sowing. In the 2nd year, mulch was also applied after harvest.

the CT treatment, which increased the surface roughness of the soil. After mulch application, the surface albedo increased in the dark-coloured yellowish-brown clayey xanthic Ferralsol at UZF and, conversely, decreased in the light-coloured red sandy soil at DTC. Throughout the two cropping years, the xanthic Ferralsol at UZF presented a lower average surface albedo than did the abruptic Lixisol at DTC (Table 1). At both sites, the surface albedo was generally greater during the dry season, when the soil was bare and dry, than during the growing season.

3.1.1. *The surface albedo values during the growing season*

At UZF, during the growing season of the first cropping year (2021/22), the highest surface albedo values were recorded at the peak of plant growth (measured by the plant area index, or PAI) for all the treatments. Although there was statiscally non-significant difference in albedo between NT and CT during this season due to similar crop development, the NTM treatment displayed higher albedo values as a result of more developed crops (Table 1). During the growing season of the second cropping year (2022/23), the albedo reached its peak value during the maize senescence phase (Fig. 2C). Across all three treatments, the surface albedo remained similar during this season due to the uniform crop growth (Fig. 2D).

At DTC, the average surface albedo during the growing seasons of the two consecutive copping years was significantly greater in the NT treatment than in the NTM and CT treatments (Table 1). For NT, the albedo values ranged from 0.15 to 0.30, whereas the albedo values of the NTM and CT treatments ranged from 0.14 to 0.23 and 0.16–0.28, respectively. Despite these differences in albedo, the NT and NTM treatments were associated with lower crop development (Fig. 2 B, C) than the CT treatment was, particularly at maximum development for both growing seasons.

3.1.2. *Surface albedo values during fallow periods*

During the dry fallow periods, the surface albedo was generally greater than that during the growing season at both UZF and DTC (Fig. 2). This was particularly obvious at DTC, where the albedo of the bare sandy soil exceeded that of the maize stands. At UZF, the presence of mulch in the NTM treatment slightly increased the surface albedo, whereas at DTC, the mulch had the opposite effect, reducing the albedo of the sandy soil. The overall difference in albedo between treatments during the fallow periods was more pronounced at DTC, where the NT treatment consistently presented a significantly higher albedo than both the CT and NTM treatments (Table 1).

After the maize harvest, the surface albedo increased for all the treatments at both sites in both cropping years (Table S2). At DTC, this postharvest increase in albedo was most noticeable in the CT treatment. When mulch was reintroduced in the NTM treatment after harvest in the second cropping year, the effect on albedo differed among the sites. At DTC, mulch significantly reduced the albedo, whereas at UZF, it led to a slight increase.

3.2. *Crop growth effect on surface albedo*

Fig. 2B and D show the PAI dynamics during both cropping years at both sites. The PAI dynamics indicate that crop growth was greater at UZF than at DTC. At UZF, the PAI dynamics were similar between the treatments during the growing seasons of both cropping years. Slightly higher maximum PAI values were observed for the NTM treatment than for the CT and NT treatments (Table 2). In contrast, at DTC, significant differences in the PAI dynamics between treatments were observed. During both growing seasons, the average PAIs were significantly greater under CT than under NT and NTM. These findings indicate that, compared with the CT treatment, the latter two treatments resulted in less crop growth. Furthermore, crop growth was lower in the second cropping year (2022/23) than in the first cropping year (2021/22) (Table 2). The GFCC experienced the same dynamics as the PAI for each

Table 1
Mean surface albedo values during the growing seasons (i.e., from maize emergence to harvest); the fallow periods (i.e., the dry seasons, when the soil is bare or covered by only crop residues) and the cropping years (i.e., the whole period from October to the following October, including both the growing and bare fallow periods).

Site		UZF									DTC								
Seasons	Treatments	Growing Season			Fallow period			Cropping year			Growing Season			Fallow period			Cropping year		
		Mean	SD	Sig.	Mean	SD	Sig.	Mean	SD	Sig.	Mean	SD	Sig.	Mean	SD	Sig.	Mean	SD	Sig.
2021/22	CT	0.15	0.020		0.18	0.020	***	0.17	0.020	*	0.19	0.030	***	0.26	0.030	***	0.23	0.05	***
	NT	0.15	0.020		0.19	0.020	**	0.17	0.030	*	0.21	0.030	***	0.29	0.030	***	0.25	0.05	***
	NTM	0.16	0.020	**	0.18	0.020	**	0.17	0.020		0.19	0.040	**	0.25	0.040	***	0.22	0.04	***
2022/23	CT	0.15	0.010		0.17	0.010	***	0.16	0.020	*	0.20	0.030	***	0.29	0.040	***	0.24	0.05	***
	NT	0.15	0.020		0.19	0.020	**	0.17	0.020	*	0.22	0.030	***	0.32	0.040	***	0.27	0.05	***
	NTM	0.15	0.020		0.18	0.020	**	0.17	0.020		0.19	0.020	**	0.26	0.030	***	0.22	0.04	***

CT: Conventional tillage, NT: No-tillage, NT: No-tillage and mulch. In 2022/23, mulch was also applied after harvest and was present during the fallow period. The errors represent standard deviations: N = 157 for the growing season 2021/22 at DTC, N = 154 for the growing season 2021/22 at UZF, N = 141 for the growing season 2022/23 at DTC, N = 138 for the growing season 2022/23 at UZF, N = 210 for the fallow period 2021/22 at DTC, N = 215 for the fallow period 2021/22 at UZF, N = 226 for the fallow period 2022/23 at DTC, N = 232 for the fallow period 2022/23 at UZF, N = 365 for the cropping years 2021/22 and 2022/23 at DTC, and N = 365 for the cropping years 2021/22 and 2022/23 at UZF. Sig. represents p-values showing level of significance among mean values for each treatments: ***$p < 0.001$; **$p < 0.01$; *$p < 0.05$,.: $p < 0.01$.

Table 2
Maximum PAI (± standard deviation, N = 6) and green fractional canopy cover (± standard deviation, N = 4) during 2 successive cropping years at the Domboshawa training center (DTC) and University of Zimbabwe farm (UZF). CT: Conventional tillage, NT: No-tillage, NTM: No-tillage and mulch.

		DTC		UZF	
Cropping year	Treatment				
2021/22		PAI max (m^2 m^{-2})	GFCC max (%)	PAI max (m^2 m^{-2})	GFCC max (%)
	CT	2.30 (±0.7)	75 (±4.35)	2.04 (±0.3)	73 (± 2.57)
	NT	0.94 (±0.3)	37 (±3.54)	1.99 (±0.6)	72 (±3.12)
	NTM	1.25 (±0.5)	46 (±2.03)	2.14 (±0.5)	78 (±4.22)
2022/23					
	CT	1.43 (±0.4)	44 (±3.62)	2.08 (±0.7)	65 (±2.52)
	NT	0.78 (±0.2)	21 (±1.4)	2.16 (±0.6)	64 (±7.08)
	NTM	0.84 (±0.3)	29 (±2.63)	2.20 (±0.6)	66 (±8.7)

site and treatment (Figure S2).

Fig. 3 shows the changes in surface albedo during the growing seasons in relation to the PAI dynamics across sites and treatments. In the first cropping year, an increase in surface albedo was observed with crop growth, levelling off upon reaching the maximum PAI. With the beginning of senescence, the surface albedo presumably decreased due to changes in leaf properties (e.g., angle and colour). The nature of this relationship can be described as a "hysteresis" effect. (See Fig. 3).

The results for the second cropping year were slightly different, and the hysteresis effect was not observed. Overall, less crop growth with less soil cover was observed than in the first cropping year (Table 2). As a consequence, the GFCC was lower at both sites, particularly for the NT and NTM treatments. The lower canopy cover in the second cropping year explains why the surface albedo dynamics were driven mostly by the soil albedo rather than by crop vegetation.

3.3. *Effect of topsoil moisture on daily surface albedo*

Fig. 2A and C (dashed lines) illustrate the dynamics of the topsoil (0–1 cm) water content during both seasons at both sites. At UZF, the topsoil moisture in the CT treatment was greater than for the NT and NTM treatments during the growing season (Fig. 2A). After harvest at the end of the rainy season, a decrease in topsoil moisture was observed. During this period, the soil moisture in NT was slightly greater than that in the CT and NTM treatments. However, at DTC, the topsoil moisture was higher in the NTM treatment during both growing seasons (Fig. 2C). After harvest, there was no significant difference between the treatments in the first cropping year. In the second cropping year, the soil moisture after harvest was significantly greater in the CT and NTM treatments than in the NT treatment.

The topsoil moisture and surface albedo were negatively correlated at both sites, especially during the bare fallow periods (Fig. 4). During the bare fallow periods, rainfall events increased the topsoil moisture, which decreased the soil albedo until the topsoil dried out again, causing the albedo to return to a value close to that before the rain. With respect to crop growth, the effects of rainfall events on the soil albedo were less pronounced, particularly when the PAI was above 1 m^2 m^{-2}. Strong and significant relationships ($p < 2.2e^{-}16$) were found for the three treatments at each site. At DTC, the strongest correlation was observed in the CT treatment, with R^2 values of 0.80 and 0.84 in the first and second cropping years, respectively. For the NT and NTM treatments, the correlations were lower but significant, with R^2 values of 0.67 and 0.51 in the first cropping year and 0.72 and 0.71 in the second cropping year, respectively. At UZF, the highest correlation was observed for the CT treatment in the first cropping year, with an R^2 of 0.79, whereas the R^2 values were 0.73 and 0.71 for the NT and NTM treatments, respectively. The correlation between surface albedo and topsoil moisture was highest during the bare fallow periods and weakened with increasing

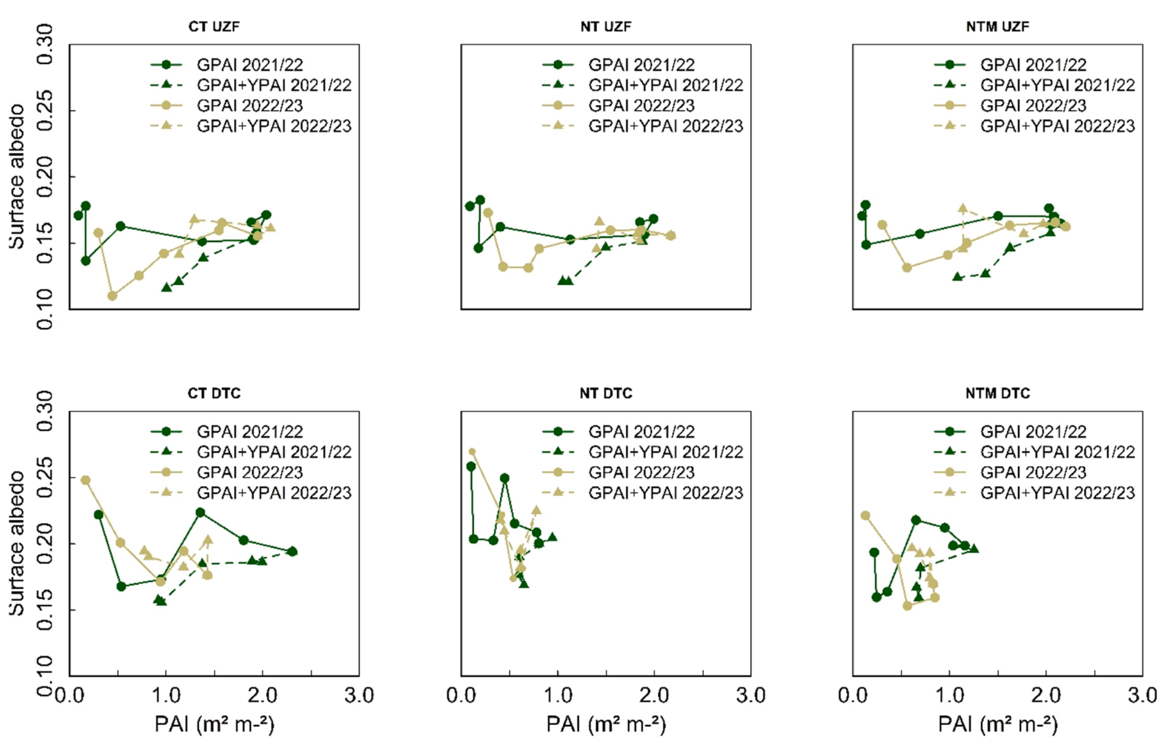

Fig. 3. Dynamics of the surface albedo as a function of the plant area index (PAI). The dot solid lines correspond to the maize growing phase with only the green PAI (labelled "GPAI"), and the triangle dashed lines correspond to the senescence phase, during which the leaves have both green and yellow tissues (labelled "GPAI + YPAI" with YPAI standing for yellow PAI). The green colour represents the 2021/22 season, and the light khaki colour represents the 2022/23 season.

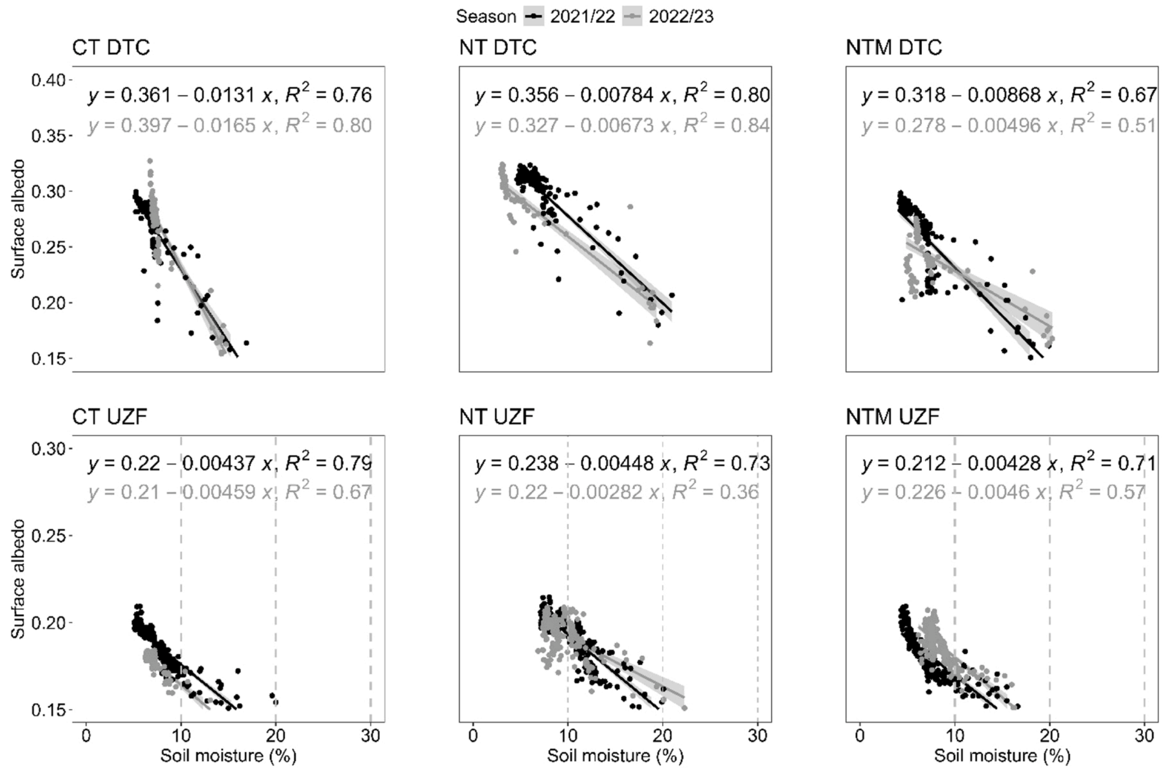

Fig. 4. Correlations between topsoil moisture (1 cm soil depth) and surface albedo on a xanthic Ferralsol (top, University of Zimbabwe farm (UZF)) and on an abruptic Lixisol (top, Domboshawa training center (DTC)) and for CT: conventional tillage, NT: no-tillage, NT: no-tillage and mulch. The data are shown for the periods between soil preparation for sowing and emergence and after harvest until the next soil preparation of the following cropping season.

crop growth. We also observed correlations between surface albedo and soil moisture at depths of 10 and 20 cm, although these were weaker than those found for topsoil moisture (Figures S5 & S6).

3.4. Radiative forcing, thermal radiation and topsoil temperature

3.4.1. Daily instantaneous radiative forcing (iRF)

At UZF, the daily iRFs for NT showed a cooling effect compared to CT throughout most of the growing season and the entire bare fallow period (Fig. 5). The average iRFs were -0.83 ± 0.17 W/m² in the first cropping year (2021/22) and -1.43 ± 0.7 W/m² in the second year (2022/23). The NTM treatment led to a cooling effect during the two successive growing seasons and to a warming effect during the first fallow period. On an annual basis, the mean iRFs of the NTM treatment were -0.43 ± 0.09 W m^{-2} during the first cropping year and -1.03 ± 0.21 W m^{-2} during the second cropping year. The mulch was applied after harvest in

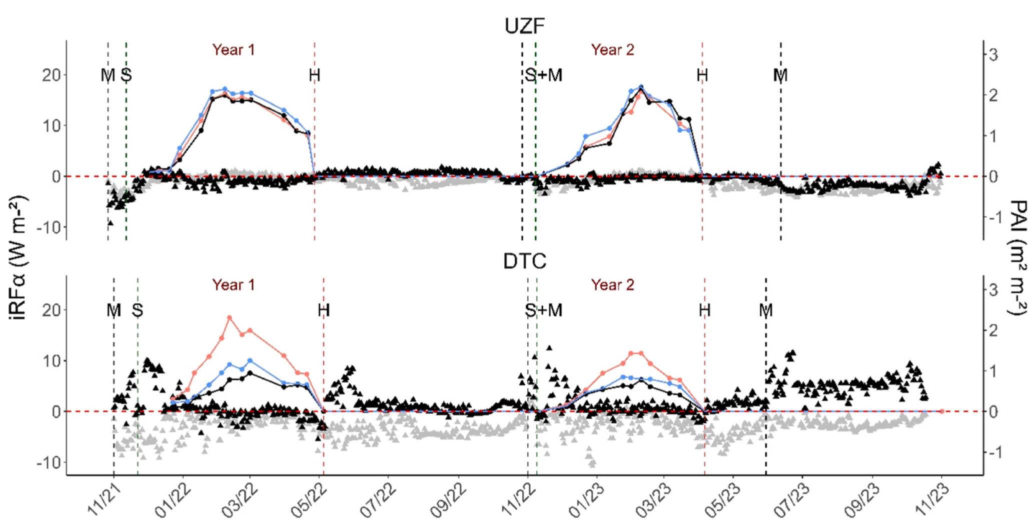

Fig. 5. Daily instantaneous radiative forcing (iRF) of no-tillage (NT, grey triangles) and no-tillage with mulch (NTM, black triangles) systems compared with conventional tillage (CT) systems. Interpolated dots represent the dynamics of the plant area index (PAI) in the three treatments: CT in salmon, NT in green, and NTM in blue. The green and red vertical dashed lines represent the sowing (S) and harvest (H) dates, respectively. The black dashed line represents the mulch (M) application date. The solid vertical dark line represents the end of the first cropping year and the beginning of the second cropping year. Tillage and mulching in the first cropping year were completed before the beginning of the measurements. Tillage and the 1st mulch application during the second cropping year were completed at maize sowing. In the 2nd cropping year, mulch was also applied after maize harvest.

the second cropping year (2022/23), increasing the surface albedo and subsequently increasing the cooling effect during the bare fallow period by -0.60 ± 0.1 W m^{-2}.

At DTC, negative daily iRF values were observed under NT relative to those under CT in both cropping years. This cooling effect was greater during the bare fallow period than during the growing season, with mean annual iRF values of -3.34 ± 0.69 W m^{-2} and -2.78 ± 0.77 W m^{-2} in the first (2021/22) and second (2022/23) cropping years, respectively. Under the NTM treatment, a positive iRF relative to the CT treatment was observed during the bare fallow periods and at the early crop development stage. During the later stages of crop growth, negative iRF values were observed. The resulting mean iRF values were 1.14 ± 0.21 W m^{-2} for the first cropping year and 2.77 ± 0.41 W m^{-2} for the second cropping year. The application of mulch after harvest in the second cropping year increased the iRF by 1.64 ± 0.11 W m^{-2}.

3.4.2. *Daily outgoing longwave (LW_{out}) radiation and topsoil temperature*

Fig. 6A shows the LW_{out} dynamics during the two successive cropping years at UZF. At this site, the daily LW_{out} values for the NT and NTM treatments were very similar to those for the CT treatment before and during the growing season. However, after mulch application following maize harvest in 2023 (see Fig. 6A), a decrease in LW_{out} was observed for the NTM treatment, whereas the LW_{out} dynamics under the NT treatment remained similar to those under the CT treatment. The mean LW_{out} values during the bare fallow period under the NT and CT treatments were 485 and 486 W m^{-2}, respectively. Compared with the CT and NT treatments, the NTM treatment had a lower LW_{out} value because of the buffering effect of the mulch layer, with an average LW_{out} value of 480 W m^{-2} during the whole fallow period. With similar crop growth between treatments (see Fig. 2B), no significant differences in LW_{out} were observed between treatments during the growing season in 2022/

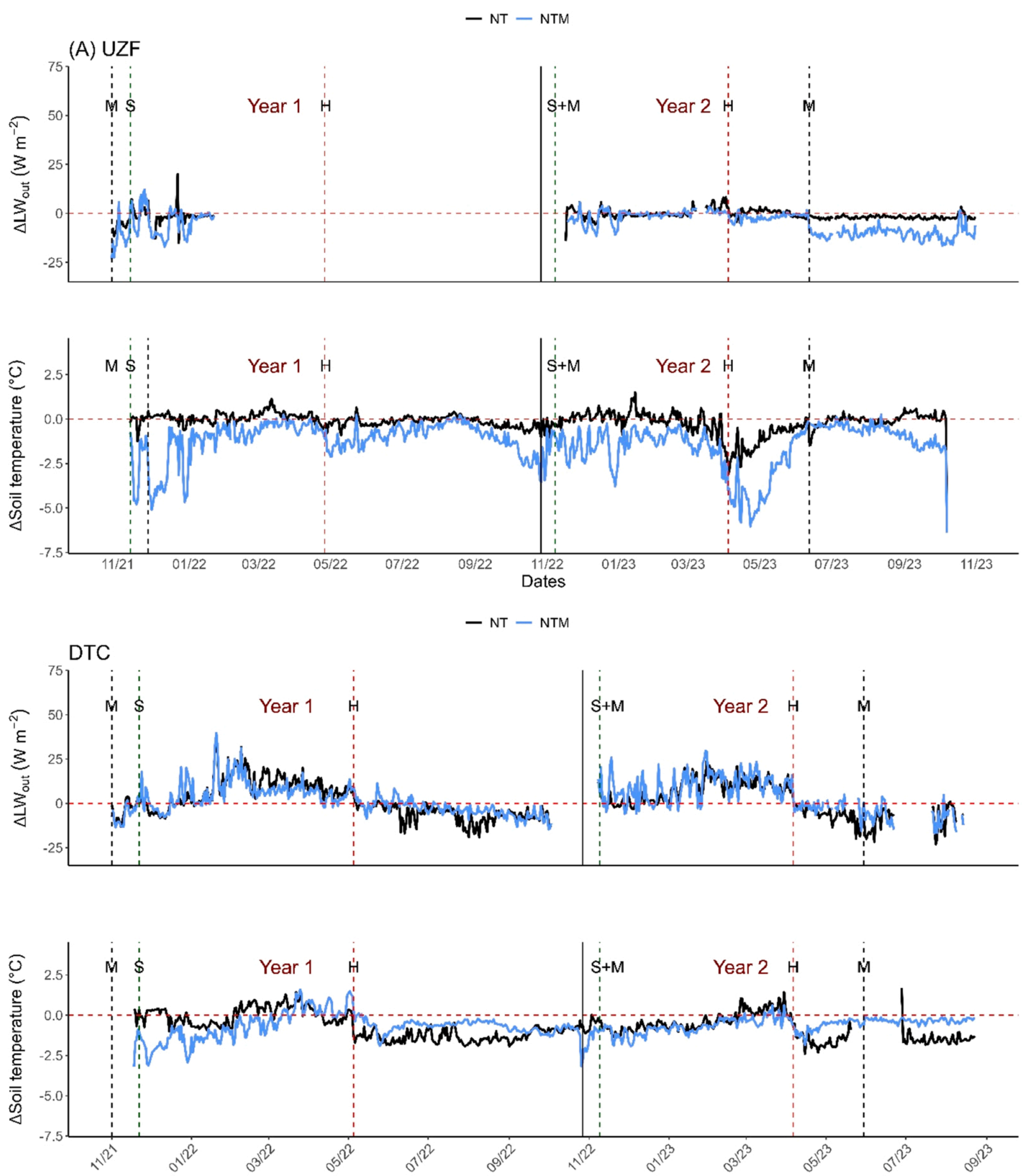

Fig. 6. Dynamics of outgoing longwave radiation dynamics (LW_{out}) (A, B, top) between no-tillage (NT) and conventional tillage (CT) (green lines) and between no-tillage with mulch (NTM) and CT (blue lines) at the UZF and DTC sites. Topsoil temperatures at 1 cm(A, B, bottom) during two cropping years (2021/22 and 2022/23) between NT and CT (green lines) and between NTM and CT (blue lines). The green and red dashed lines represent the sowing (S) and harvest (H) dates, respectively. The black dashed line represents the mulch (M) application date. The solid vertical dark line represents the end of the first cropping year and the beginning of the second cropping year. Tillage and mulching in the first cropping year were performed before the beginning of the measurement. Tillage and 1st mulch application during the second cropping year were performed at sowing. Mulch was also applied after harvest.

23. During this period, the mean LW_{out} values were 461 W m^{-2} for NT and CT and 460 W m^{-2} for NTM.

At UZF, no significant differences were detected in the topsoil (0–1 cm) temperature dynamics between the NT and CT treatments during the first (2021/22) and second (2022/23) cropping years (Fig. 6B). In the second cropping year, a rapid decrease in temperature was observed under the NT treatment compared with the CT treatment immediately after maize harvest. The surface temperature was lower under the NTM treatment than under the CT treatment because the mulch covered the soil before sowing, during crop growth and after maize harvest during the second cropping year. Similar observations were made in the second cropping year, with a 5 °C difference between the NTM and CT treatments just after the maize harvest. The cooling observed in the NTM treatments can partially explain the differences in LW_{out} between the NTM treatment and the CT and NT treatments.

At DTC, the daily LW_{out} values were very similar between the treatments during the bare fallow periods in both cropping years (Fig. 6C), with values of 458 W m^{-2} and 475 for NT and 464 W m^{-2} and 481 W m^{-2} for CT in the first and second cropping years, respectively. In contrast, during the growing season, the differences in LW_{out} were significant between the CT and NT treatments and between the CT and NTM treatments due to greater crop growth under the CT treatment. During the growing season, the mean LW_{out} values under NT compared with those under CT were 464 vs. 455 W m^{-2} and 468 vs. 460 W m^{-2} during the first and second cropping years, respectively. The small difference in LW_{out} between the NT and CT treatments during crop growth was due to the lower PAI resulting from poorer crop growth. During the bare fallow period, the mean LW_{out} values for the NTM treatment were 461 and 437 W m^{-2} in the first and second cropping years, respectively. Compared with the CT treatment, the NTM treatment resulted in poorer crop growth, resulting in average LW_{out} values of 462 W m^{-2} and 470 W m^{-2}, whereas the LW_{out} values of the first and second growing seasons were 455 W m^{-2} and 460 W m^{-2}, respectively.

In both cropping years, the topsoil temperatures were generally similar between the NT and CT treatments during crop growth periods, except during the early stages of crop growth in the first cropping year (Fig. 6D). However, lower daily topsoil temperatures were observed after maize harvest in the NT treatment than in the CT treatment during both cropping years. The daily topsoil temperatures were significantly lower in the NTM treatment than in the CT treatment during the early stages of crop growth and throughout the cropping year, probably because of the buffering effect of the mulch layer on the soil temperature.

4. Discussion

4.1. Interactive effects of soil type and cropping system on the dynamics of the surface albedo

In this study, we showed that no-tillage and maize residue mulching can have significant effects on the surface albedo dynamics and on the longwave radiation from the soil surface. While no-tillage generally increases the soil albedo due to the lower soil surface roughness, mulch either increases or decreases the surface albedo depending on the soil surface properties.

We observed that the brightness of the soil surface modulates the effects of mulching and no-tillage on the surface albedo and iRF. In a previous work, Post et al. (2000) reported that soil surface colour is an important driver of the surface albedo. Horton et al. (1996) also reported that the albedo of light-coloured crop residues may be greater than that of dark-coloured yellow-brown soil; therefore, a layer of crop residues can reduce the soil surface reflectance.

Soil colour is determined by several factors, such as the organic carbon content. At our experimental sites, the soil organic carbon contents were measured as described by Shumba et al. (2024). In the topsoil layer (0–5 cm) of the abruptic Lixisol (DTC), the soil organic carbon contents were 0.6 g C kg^{-1} for the CT and NT treatments, whereas for the NTM treatments, the contents was 0.8 g C kg^{-1}. In xanthic Ferralsol (UZF), the soil organic carbon contents was higher, at 1.80 g C kg^{-1} for CT, 1.85 g C kg^{-1} for NT and 2.1 g C kg^{-1} for NTM (Shumba et al., 2024). Mineral components such as iron oxides also determine soil colour (Cierniewski et al., 2018). For example, a field study by Rosenberg et al. (1983) demonstrated the contrast between a dry sandy soil with albedo values ranging between 0.25 and 0.45 and a dark soil with albedo values ranging between 0.16 and 0.17, which aligns with the observations in the soils of our study. At DTC, the mulch on a clear sandy soil therefore reduced the surface albedo, whereas at UZF, the maize residues increased the surface albedo. In southeastern France, Davin et al. (2014) also reported that the mulch of crop residues on no-tilled loamy soil increased the surface albedo (by approximately 0.1) compared with tilled soils without mulch.

At DTC, we observed that the surface albedo in the NTM treatment was lower than in the other treatments, even before mulch application at sowing and after harvest (the mulch decomposed at that time), when the soil rugosity was comparable among the treatments. The reason is likely that the annual mulch application at this site slightly increased the soil organic carbon content by 0.25 g C kg^{-1} and 0.30 g C kg^{-1} compared with the NT and CT treatments, respectively (Shumba et al., 2024). The climate benefit associated with soil organic carbon sequestration was therefore partly or totally counterbalanced by the positive iRF effect induced by the soil darkening effect (Post et al., 2000). In another study, Pique et al. (2023) reported a significant risk of losing part of the climate benefit of soil organic carbon sequestration through soil albedo darkening effects if soils are not permanently covered once carbon farming practices are implemented.

Soil roughness also affects the surface albedo and its dynamics between treatments (e.g., CT vs. NT), especially under dry conditions, which corroborates previous findings under similar pedo-climatic conditions in West Africa (Oguntunde et al., 2006). At our sites, we observed differences in the surface albedo between the CT and NT treatments after soil preparation for maize sowing at UZF and between the CT and NT treatments at DTC during the bare fallow period. At UZF, the difference in surface albedo between the NT and CT treatments before sowing could be caused by tillage, which increases the surface roughness, causing more incident solar radiation to be trapped and reducing the surface albedo, as shown in previous studies (Cierniewski et al., 2015; Matthias et al., 2000; Oguntunde et al., 2006). At DTC, the difference between the NT and CT treatments during the bare fallow period could be explained by the presence of surface soil crusts in the NT treatment, which were absent in the CT treatment. In addition, before sowing, the surface soil layer in the NT treatment was smooth and very bright compared with that in the CT treatment. In contrast, the difference in soil roughness between the CT and NT treatments was very small after the maize harvest and during the following fallow period.

4.2. Effects of maize growth on surface albedo dynamics

According to Hatfield and Carlson (1979) and Breuer et al. (2003), the albedo of maize varies between 0.16 and 0.25 across varieties. However, due to the light-coloured red sandy soil at the DTC, the high surface albedo value of 0.21 in the NT treatment during the maize growing season was due to weak maize growth and vegetation cover (Table 2). In contrast, low surface albedo values of 0.19 during the growing season were observed in the CT treatment, which was characterized by better development of the maize stand than the NT treatment; this means that at this site, the surface albedo of the maize stand was lower than that of the bare soil. Several studies in temperate regions have, however, shown the opposite: soil coverage by cover crops leads to increases in surface albedo compared with bare fallow soil (Carrer et al., 2018; Lugato et al., 2020; Pique et al., 2023). Exceptions were observed for light-coloured soils by Kaye and Quemada (2017) and Carrer et al. (2018).

During the two cropping years, the surface albedo values during the growing season were almost always lower than those of the bare soil surface during fallow periods in all the treatments and at both sites (Figs. 2A and 2C). The surface albedo of bare soil was strongly driven by topsoil moisture. During the growing season, the different treatments affected the surface albedo because of incomplete vegetation coverage; this suggests that the surface albedo was driven during the growing season by both crop phenology and soil moisture. The GFCC did not reach 100 % at either site (Table 2), which may explain the influence of management-induced changes in topsoil organic matter and moisture content on the surface albedo dynamics. These effects are especially pronounced at DTC, where there is low crop and foliage growth. The surface albedo values reach saturation with high PAI values and may even decline subsequently as internal reflections become more pronounced (Bsaibes et al., 2009). During the maize senescence phase, leaves wilt, which modifies both leaf colour and canopy structure. Due to the wilted leaves, the vegetation cover decreased, but the soil was shadowed more by the vegetated parts when the sun stood lower. The soil shadowing effect of plants works as a radiation trap and reduces the amount of reflected shortwave radiation (He et al., 2021; Wang et al., 2007). Another important driver of the decreased albedo during senescence is the lower reflectance and therefore lower albedo of yellow leaves than of green leaves. For example, an increase in surface albedo during the development stage and a decrease in surface albedo with senescence were observed for maize in the study of Jacobs and van Pul (1990). Oguntunde and van de Giesen (2004) reported a significant increase in albedo from emergence to maturity in maize, followed by a slight decrease during maturity due to the occurrence of yellow tissues in the plants.

4.3. Changes in iRF and LW_{out} caused by tillage and crop residue management

Changes in the surface albedo impact the amount of solar radiation that is absorbed by the Earth's surface. A reduction in surface albedo, indicating lower reflectivity, results in increased absorption of solar energy, causing local warming (Liu et al., 2022). Conversely, an increase in albedo, signifying higher reflectivity, results in diminished absorption and induces cooling (Carrer et al., 2018). In both the light-coloured red sandy soil at DTC and the dark-coloured yellow-brown clayey soil at UZF, the systematic cooling effect of NT compared with that of CT is explained by a greater albedo during both the growing season and the bare fallow periods. According to Davin et al. (2014), no-tillage without mulch in European croplands caused a global cooling effect and, locally, decreased surface temperatures during heatwave events. This local attenuation of heatwaves makes no-tillage practices an interesting climate adaptation strategy (Seneviratne et al., 2018). A modelling study by Lobell et al. (2006) further demonstrated the potential impact that no-tillage could have on the climate if applied globally; they estimated a reduction in the global mean temperature of approximately 0.2 °C (Lobell et al., 2006), which is quite substantial.

At the DTC, the application of mulch led to a decrease in the surface albedo. Compared with bare sandy soil, mulch has a lower albedo at this site, leading to a decrease in the surface albedo and a positive iRF in the NTM treatment. In contrast, at UZF, the soil surface has a darker colour than mulch does, which results in a cooling effect through mulching. However, the benefit of mulching on the local temperature regime could be significantly offset by other effects, namely, a reduction in the evaporation flux, an increase in surface temperature, and an increase in the sensible heat flux (Davin et al., 2014).

The other important biophysical effect that is induced by no-tillage and crop residue management involves the modification of topsoil temperatures and, consequently, the longwave radiation emitted (Breil et al., 2023; Bright et al., 2017; Donohoe et al., 2014). The DTC site experienced a significant difference in longwave radiation emitted from NT and NTM compared to CT during the growing season. This difference can be explained by the better crop growth in the CT treatment than in the other two treatments. As a result, evaporation was likely greater in the CT treatment than in the CT and NT treatments, and this process can reduce the soil temperature and longwave radiation emitted by the surface during the growing season. For example, Ceschia et al. (2017) demonstrated that the albedo-induced cooling effect of cover crops could be magnified when their effects on longwave radiation and the Bowen ratio (i.e., the ratio of sensible heat flux to latent heat flux near the surface) are accounted for. Furthermore, the authors highlighted that cover crops caused, on average, a 2.5 °C decrease in local topsoil temperature compared with the bare soil treatment, which could have slowed organic matter mineralization.

4.4. Limitations and perspectives

Continuous monitoring of the albedo, surface temperature and LW_{out} helped us to better understand the biophysical effects of CA practices and their consequences for climate change mitigation. The detailed information collected in this study contributes to a better assessment of the climatic impact of land management and can be fed into soil—crop models or Earth system models for better simulations of the impacts beyond the field scale. However, changes in management practices affect the local climate not only through albedo effects on iRF or through changes in LW_{out} but also through other biogeophysical processes, such as changes in evapotranspiration, sensible vs. latent heat fluxes and soil water content (Idso et al., 1975; O'Brien and Daigh, 2019; Rost and Mayer, 2006) and through biogeochemical effects (changes in soil organic carbon and greenhouse gas emissions) (Powlson et al., 2016). In our study, we did not conduct an analysis of the changes in latent or sensible heat fluxes to investigate the effect of management on energy partitioning at the surface (Davin et al., 2014; Ceschia et al., 2017). However, complementary studies have been conducted on soil organic carbon storage and greenhouse gas emissions (Shumba et al., 2023, 2024) at our sites. The results of these studies provide the opportunity to compare the biogeophysical and biogeochemical effects of CA practices to estimate their net climatic impact; this will be investigated in our next study, which will compare these effects both in the short term and in the long term. Modelling efforts would be valuable for exploring aspects that were not investigated in this study, such as management effects on the partitioning between sensible and latent heat fluxes. Coupled surface—atmosphere modelling, which incorporates feedback effects, is essential for assessing the net climatic impact of CA practices on regional and global climates.

5. Conclusion

Based on in situ measurements, we studied how the soil type, soil moisture, crop growth and management practices impact the surface albedo and longwave radiation dynamics, as well as subsequent instantaneous radiative forcing. Independent of the soil type, the no-tillage treatment increased the surface albedo compared with conventional tillage; this resulted in a systematic albedo cooling effect due to no-tillage practices during both the growing season and the bare fallow period. However, the retention of crop residues has different effects on the surface albedo depending on the soil type. In bright sandy soil (abruptic Lixisol), the surface albedo decreased, leading to positive instantaneous radiative forcing with a warming effect, whereas in darker soil (xanthic Ferralsol), the surface albedo increased, leading to a cooling effect. For a given practice, the biogeophysical effects and impacts on climate are therefore very context specific. These effects are not negligible and should be considered together with the biogeochemical effects of CA practices to establish more efficient climate mitigation strategies.

CRediT authorship contribution statement

Christian Thierfelder: Writing – review & editing, Resources, Funding acquisition. **Regis Chikowo:** Writing – review & editing, Funding acquisition. **Marc Corbeels:** Writing – review & editing, Writing – original draft, Project administration, Funding acquisition. **François Affholder:** Writing – review & editing, Writing – original draft, Project administration, Funding acquisition. **Frédéric Baudron:** Writing – review & editing, Writing – original draft, Funding acquisition. **Eric Ceschia:** Writing – review & editing, Writing – original draft, Visualization, Validation, Supervision, Software, Methodology, Investigation, Funding acquisition, Formal analysis, Data curation, Conceptualization. **DIOP Souleymane:** Writing – review & editing, Writing – original draft, Visualization, Validation, Supervision, Software, Methodology, Investigation, Formal analysis, Data curation, Conceptualization. **Rémi Cardinael:** Writing – review & editing, Writing – original draft, Visualization, Validation, Supervision, Software, Resources, Project administration, Methodology, Investigation, Funding acquisition, Formal analysis, Data curation, Conceptualization. **Ronny Lauerwald:** Writing – review & editing, Writing – original draft, Visualization, Validation, Supervision, Methodology, Investigation, Formal analysis, Data curation, Conceptualization. **Morgan Ferlicoq:** Writing – review & editing, Writing – original draft, Methodology, Conceptualization.

Declaration of Competing Interest

The authors declare the following financial interests/personal relationships which may be considered as potential competing interests: Souleymane DIOP reports financial support was provided by European commission and CLAND convergence institute. Rémi Cardinael reports financial support (equipment) was provided by MAIZE CGIAR research program. If there are other authors, they declare that they have no known competing financial interests or personal relationships that could have appeared to influence the work reported in this paper.

Acknowledgement

Authors are grateful to the International Maize and Wheat Improvement Center (CIMMYT) and the MAIZE CGIAR Research Program (www.maize.org) for funding the ACCURATE "Albedo, Conservation agriCUltuRe and climATe bEnefit" project, to the CLAND Convergence Institute with contributions of the Agence Nationale de la Recherche (ANR) grant ANR-16-CONV-0003 (CLAND), to Cirad for the LANCELOT "aLbedo chANGe and Climate bEnefit in Land-based mitigatiOn pracTices" project, and to the European Union for funding the RAIZ "Promoting agroecological intensification for resilience building" project FOOD/2021/424–933 (https://raiz.org.zw/). The authors would also like to thank CIMMYT field workers for their assistance in the field work.

Appendix A. Supporting information

Supplementary data associated with this article can be found in the online version at doi:10.1016/j.still.2025.106804.

Data availability

Data are freely available on the Cirad data repository.

References

Akbari, H., Menon, S., Rosenfeld, A., 2009. Global cooling: increasing world-wide urban albedos to offset CO_2. Clim. Change 94, 275–286. https://doi.org/10.1007/s10584-008-9515-9.

Andrews, T., Betts, R.A., Booth, B.B.B., Jones, C.D., Jones, G.S., 2017. Effective radiative forcing from historical land use change. Clim. Dyn. 48, 3489–3505. https://doi.org/10.1007/s00382-016-3280-7.

Aydinalp, C., Cresser, M.S., 2008. The effects of global Climate Change on agriculture. J. Agric. Env. Sci. 672–676.

Beillouin, D., Corbeels, M., Demenois, J., Berre, D., Boyer, A., Fallot, A., Feder, F., Cardinael, R., 2023. A global meta-analysis of soil organic carbon in the anthropocene. Nat. Commun. 14, 3700. https://doi.org/10.1038/s41467-023-39338-z.

Bellouin, N., Davies, W., Shine, K.P., Quaas, J., Mülmenstädt, J., Forster, P.M., Smith, C., Lee, L., Regayre, L., Brasseur, G., Sudarchikova, N., Bouarar, I., Boucher, O., Myhre, G., 2020. Radiative forcing of climate change from the copernicus reanalysis of atmospheric composition. Earth Syst. Sci. Data 12, 1649–1677. https://doi.org/10.5194/essd-12-1649-2020.

Betts, R.A., 2000. Offset of the potential carbon sink from boreal forestation by decreases in surface albedo. Nature 408, 187–190. https://doi.org/10.1038/35041545.

Béziat, P., 2009. Effets Des Conditions Environnementales Et Des Pratiques Culturales Sur Les Flux De Carbone Et D'eau Dans Les Agrosystèmes (phd). Université de Toulouse, Université Toulouse III - Paul Sabatier.

Béziat, P., Rivalland, V., Tallec, T., Jarosz, N., Boulet, G., Gentine, P., Ceschia, E., 2013. Evaluation of a simple approach for crop evapotranspiration partitioning and analysis of the water budget distribution for several crop species. Agric. For. Meteorol. 177, 46–56. https://doi.org/10.1016/j.agrformet.2013.03.013.

Breil, M., Krawczyk, F., Pinto, J.G., 2023. The response of the regional longwave radiation balance and climate system in Europe to an idealized afforestation experiment. Earth Syst. Dyn. 14, 243–253. https://doi.org/10.5194/esd-14-243-2023.

Breuer, L., Eckhardt, K., Frede, H.-G., 2003. Plant parameter values for models in temperate climates. Ecol. Model. 169, 237–293. https://doi.org/10.1016/S0304-3800(03)00274-6.

Bright, R.M., Davin, E., O'Halloran, T., Pongratz, J., Zhao, K., Cescatti, A., 2017. Local temperature response to land cover and management change driven by non-radiative processes. Nat. Clim. Change 7, 296–302. https://doi.org/10.1038/nclimate3250.

Bright, R.M., Lund, M.T., 2021. CO_2-equivalence metrics for surface albedo change based on the radiative forcing concept: a critical review. Atmos. Chem. Phys. 21, 9887–9907. https://doi.org/10.5194/acp-21-9887-2021.

Bsaibes, A., Courault, D., Baret, F., Weiss, M., Olioso, A., Jacob, F., Hagolle, O., Marloie, O., Bertrand, N., Desfond, V., Kzemipour, F., 2009. Albedo and LAI estimates from FORMOSAT-2 data for crop monitoring. Remote Sens. Environ. 14.

Cai, H., Wang, J., Feng, Y., Wang, M., Qin, Z., Dunn, J.B., 2016. Consideration of land use change-induced surface albedo effects in life-cycle analysis of biofuels. Energy Environ. Sci. 9, 2855–2867. https://doi.org/10.1039/C6EE01728B.

Carrer, D., Pique, G., Ferlicoq, M., Ceamanos, X., Ceschia, E., 2018. What is the potential of cropland albedo management in the fight against global warming? A case study based on the use of cover crops. Environ. Res. Lett. 13, 044030. https://doi.org/10.1088/1748-9326/aab650.

Ceschia, E., Mary, B., Ferlicoq, M., Pique, G., Carrer, D., Dejoux, J.-F., dedieux, gérard, 2017. Potentiel d'atténuation des changements climatiques par les couverts intermédiaires. Innov. Agron.

Cierniewski, J., Ceglarek, J., Kaźmierowski, C., 2018. Estimating the diurnal blue-sky albedo of soils with given roughness using their laboratory reflectance spectra. J. Quant. Spectrosc. Radiat. Transf. 217, 213–223. https://doi.org/10.1016/j.jqsrt.2018.06.003.

Cierniewski, J., Karnieli, A., Kazmierowski, C., Królewicz, S., Piekarczyk, J., Lewińska, K., Goldberg, A., Wesolowski, R., Orzechowski, M., 2015. Effects of soil surface irregularities on the diurnal variation of soil broadband Blue-Sky albedo. IEEE J. Sel. Top. Appl. Earth Obs. Remote Sens. 8. https://doi.org/10.1109/JSTARS.2014.2330691.

Cierniewski, J., Karnieli, A., Kuśnierek, K., Goldberg, A., Herrmann, I., 2013. Approximating the average daily surface albedo with respect to soil roughness and latitude. Int. J. Remote Sens. 34, 3416–3424. https://doi.org/10.1080/01431161.2012.716530.

Corbeels, M., Cardinael, R., Powlson, D., Chikowo, R., Gerard, B., 2020. Carbon sequestration potential through conservation agriculture in Africa has been largely overestimated comment on: "meta-analysis on carbon sequestration through conservation agriculture in Africa. Soil Tillage Res. 196, 1–3. https://doi.org/10.1016/j.still.2019.104300.

Davin, E.L., de Noblet-Ducoudré, N., 2010. Climatic impact of Global-Scale deforestation: radiative versus nonradiative processes. J. Clim. 23, 97–112. https://doi.org/10.1175/2009JCLI3102.1.

Davin, E.L., Seneviratne, S.I., Ciais, P., Olioso, A., Wang, T., 2014. Preferential cooling of hot extremes from cropland albedo management. Proc. Natl. Acad. Sci. 111, 9757–9761. https://doi.org/10.1073/pnas.1317323111.

Diop, S., 2023. Four-component net radiometers to quantify albedo and heat fluxes in conservation agriculture. Nat. Rev. Earth Environ. https://doi.org/10.1038/s43017-023-00432-x.

Donohoe, A., Armour, K.C., Pendergrass, A.G., Battisti, D.S., 2014. Shortwave and longwave radiative contributions to global warming under increasing CO2. Proc. Natl. Acad. Sci. 111, 16700–16705. https://doi.org/10.1073/pnas.1412190111.

Forster, P., Ramaswamy, Venkatachalam, Artaxo, Paulo, Berntsen, Terje, Betts, Richard, Fahey, David W., Haywood, James, Lean, Judith, Lowe, David C., Raga, Graciela, Schulz, Michael, Dorland, Robert Van, Bodeker, G., Etheridge, D., Foukal, P., Fraser, P., Geller, M., Joos, F., Keeling, C.D., Keeling, R., Kinne, S., Lassey, K., Oram, D., O'Shaughnessy, K., Ramankutty, N., Reid, G., Rind, D., Rosenlof, K., Sausen, R., Schwarzkopf, D., Solanki, S.K., Stenchikov, G., Stuber, N., Takemura, T., Textor, C., Wang, R., Weiss, R., Whorf, T., Nakajima, T., Ramanathan, V., Ramaswamy, V., Artaxo, P., Berntsen, T., Betts, R., Fahey, D.W., Haywood, J., Lean, J., Lowe, D.C., Myhre, G., Nganga, J., Prinn, R., Raga, G., Schulz, M., Dorland, R.Van, 2007. Changes in Atmospheric Constituents and in Radiative Forcing 106.

Forster, P.M., Richardson, T., Maycock, A.C., Smith, C.J., Samset, B.H., Myhre, G., Andrews, T., Pincus, R., Schulz, M., 2016. Recommendations for diagnosing effective radiative forcing from climate models for CMIP6. -12,475 J. Geophys. Res. Atmospheres 121 (12), 460. https://doi.org/10.1002/2016JD025320.

Franzluebbers, A.J., 2010. Achieving soil organic carbon sequestration with conservation agricultural systems in the southeastern United States. Soil Sci. Soc. Am. J. 74, 347–357. https://doi.org/10.2136/sssaj2009.0079.

Fu, Q., Liou, K.-N., 1993. Parameterization of the radiative properties of cirrus clouds. J. Atmos. Sci. 50, 2008–2025.

Fuentes-Ponce, M.H., Gutiérrez-Díaz, J., Flores-Macías, A., González-Ortega, E., Mendoza, A.P., Sánchez, L.M.R., Novotny, I., Espíndola, I.P.M., 2022. Direct and indirect greenhouse gas emissions under conventional, organic, and conservation agriculture. Agric. Ecosyst. Environ. 340, 108148. https://doi.org/10.1016/j.agee.2022.108148.

Hatfield, J.L., Carlson, R.E., 1979. Light quality distributions and spectral albedo of three maize canopies. Agric. Meteorol. 20, 215–226. https://doi.org/10.1016/0002-1571(79)90022-0.

He, Y., Lin, E.S., Yu, Z., Tan, C.L., Tan, P.Y., Wong, N.H., 2021. The effect of dynamic albedos of plant canopy on thermal performance of rooftop greenery: a case study in Singapore. Build. Environ. 205, 108247. https://doi.org/10.1016/j.buildenv.2021.108247.

Hirsch, A.L., Prestele, R., Davin, E.L., Seneviratne, S.I., Thiery, W., Verburg, P.H., 2018. Modelled biophysical impacts of conservation agriculture on local climates. Glob. Change Biol. 24, 4758–4774. https://doi.org/10.1111/gcb.14362.

Hirsch, A.L., Wilhelm, M., Davin, E.L., Thiery, W., Seneviratne, S.I., 2017. Can climate-effective land management reduce regional warming? J. Geophys. Res. Atmos. 122, 2269–2288. https://doi.org/10.1002/2016JD026125.

Horton, R., Bristow, K.L., Kluitenberg, G.J., Sauer, T.J., 1996. Crop residue effects on surface radiation and energy balance? Review. Theor. Appl. Clim. 54, 27–37. https://doi.org/10.1007/BF00863556.

Idso, S.B., Jackson, R.D., Reginato, R.J., Kimball, B.A., Nakayama, F.S., 1975. The dependence of bare soil albedo on soil water content. J. Appl. Meteorol. Climatol. 14, 109–113 https://doi.org/10.1175/1520-0450(1975)014<0109:TDOBSA>2.0.CO;2.

IPCC, 2018: Global Warming of 1.5°C. An IPCC Special Report on the impacts of global warming of 1.5°C above pre-industrial levels and related global greenhouse gas emission pathways, in the context of strengthening the global response to the threat of climate change, sustainable development, and efforts to eradicate poverty [Masson-Delmotte, V., P. Zhai, H.-O. Pörtner, D. Roberts, J. Skea, P.R. Shukla, A. Pirani, W. Moufouma-Okia, C. Péan, R. Pidcock, S. Connors, J.B.R. Matthews, Y. Chen, X. Zhou, M.I. Gomis, E. Lonnoy, T. Maycock, M. Tignor, and T. Waterfield (eds.)]. In Press.GIEC, 2018: Annexe I: Glossaire [Matthews, J.B.R. (éd.)]. Dans: Réchauffement planétaire de 1,5 °C, Rapport spécial du GIEC sur les conséquences d'un réchauffement planétaire de 1,5 °C par rapport aux niveaux préindustriels et les trajectoires associées d'émissions mondiales de gaz à effet de serre, dans le contexte du renforcement de la parade mondiale au changement climatique, du développement durable et de la lutte contre la pauvreté [Publié sous la direction de V. Masson-Delmotte, P. Zhai, H. O. Pörtner, D. Roberts, J. Skea, P.R. Shukla, A. Pirani, W. Moufouma-Okia, C. Péan, R. Pidcock, S. Connors, J.B.R. Matthews, Y. Chen, X. Zhou, M.I. Gomis, E. Lonnoy, T. Maycock, M. Tignor et T. Waterfield]. Sous presse.

Irmak, S., Kukal, M.S., 2022. Alteration in surface energy balance fluxes induced from long-term disk-tilled versus no-till management in maize production. Soil Tillage Res. 221, 105383. https://doi.org/10.1016/j.still.2022.105383.

Jacobs, A.F.G., van Pul, W.A.J., 1990. Seasonal changes in the albedo of a maize crop during two seasons. Agric. For. Meteorol. 49, 351–360. https://doi.org/10.1016/0168-1923(90)90006-R.

Jàuregui, J.M., Delbino, F.G., Brance Bonvini, M.I., Berhongaray, G., 2019. Determining yield of forage crops using the canopeo mobile phone app. J. NZ Grassl. 41–46. https://doi.org/10.33584/jnzg.2019.81.385.

Kassambara, A, 2023. ggpubr: "ggplot2" Based Publication Ready Plots. R package version 0.6.1. https://rpkgs.datanovia.com/ggpubr/.

Kaye, J.P., Quemada, M., 2017. Using cover crops to mitigate and adapt to climate change. A review. Agron. Sustain. Dev. 37, 4. https://doi.org/10.1007/s13593-016-0410-x.

Lenton, T.M., Vaughan, N.E., 2009. The radiative forcing potential of different climate geoengineering options. Atmos. Chem. Phys. 23.

Liang, L., Schwartz, M.D., Fei, S., 2012. Photographic assessment of temperate forest understory phenology in relation to springtime meteorological drivers. Int. J. Biometeorol. 13.

Liao, W., Liu, X., Burakowski, E., Wang, D., Wang, L., Li, D., 2020. Sensitivities and responses of land surface temperature to Deforestation-Induced biophysical changes in two global earth system models. J. Clim. 33, 8381–8399. https://doi.org/10.1175/JCLI-D-19-0725.1.

Liu, J., Desjardins, R.L., Wang, S., Worth, D.E., Qian, B., Shang, J., 2022. Climate impact from agricultural management practices in the Canadian prairies: carbon equivalence due to albedo change. J. Environ. Manag. 302, 113938. https://doi.org/10.1016/j.jenvman.2021.113938.

Lobell, D.B., Bala, G., Duffy, P.B., 2006. Biogeophysical impacts of cropland management changes on climate. L06708 Geophys. Res. Lett. 33. https://doi.org/10.1029/2005GL025492.

Lugato, E., Cescatti, A., Jones, A., Ceccherini, G., Duveiller, G., 2020. Maximising climate mitigation potential by carbon and radiative agricultural land management with cover crops. Environ. Res. Lett. 15, 094075. https://doi.org/10.1088/1748-9326/aba137.

Luyssaert, S., Jammet, M., Stoy, P.C., Estel, S., Pongratz, J., Ceschia, E., Churkina, G., Don, A., Erb, K., Ferlicoq, M., Gielen, B., Grünwald, T., Houghton, R.A., Klumpp, K., Knohl, A., Kolb, T., Kuemmerle, T., Laurila, T., Lohila, A., Loustau, D., McGrath, M. J., Meyfroidt, P., Moors, E.J., Naudts, K., Novick, K., Otto, J., Pilegaard, K., Pio, C.A., Rambal, S., Rebmann, C., Ryder, J., Suyker, A.E., Varlagin, A., Wattenbach, M., Dolman, A.J., 2014. Land management and land-cover change have impacts of similar magnitude on surface temperature. Nat. Clim. Change 4, 389–393. https://doi.org/10.1038/nclimate2196.

Mapanda, F., Mupini, J., Wuta, M., Nyamangara, J., Rees, R.M., 2010. A cross-ecosystem assessment of the effects of land cover and land use on soil emission of selected greenhouse gases and related soil properties in Zimbabwe. Eur. J. Soil Sci. 61, 721–733. https://doi.org/10.1111/j.1365-2389.2010.01266.x.

Matthias, A.D., Fimbres, A., Sano, E.E., Post, D.F., Accioly, L., Batchily, A.K., Ferreira, L. G., 2000. Surface roughness effects on soil albedo. Soil Sci. Soc. Am. J. 64, 1035–1041. https://doi.org/10.2136/sssaj2000.6431035x.

Mhlanga, B., Pellegrino, E., Thierfelder, C., Ercoli, L., 2022. Conservation agriculture practices drive maize yield by regulating soil nutrient availability, arbuscular mycorrhizas, and plant nutrient uptake. Field Crops. Res. 277, 108403. https://doi.org/10.1016/j.fcr.2021.108403.

Muñoz, I., Campra, P., Fernández-Alba, A.R., 2010. Including CO2-emission equivalence of changes in land surface albedo in life cycle assessment. Methodology and case study on greenhouse agriculture. Int. J. Life Cycle Assess. 15, 672–681. https://doi.org/10.1007/s11367-010-0202-5.

Namatsheve, T., Cardinael, R., Chikowo, R., Corbeels, M., Rugare, J.T., Mabasa, S., Ripoche, A., 2024. Do intercropping and mineral nitrogen fertilizer affect weed community structures in low-input maize-based cropping systems? Crop Prot. 176, 106486. https://doi.org/10.1016/j.cropro.2023.106486.

O'Brien, P.L., Daigh, A.L.M., 2019. Tillage practices alter the surface energy balance – a review. Soil Tillage Res. 195, 104354. https://doi.org/10.1016/j.still.2019.104354.

Oguntunde, P.G., Ajayi, A.E., Giesen, N. van de, 2006. Tillage and surface moisture effects on bare-soil albedo of a tropical loamy sand. Soil Tillage Res. 85, 107–114. https://doi.org/10.1016/j.still.2004.12.009.

Oguntunde, P., van de Giesen, N., 2004. Crop growth and development effects on surface albedo for maize and cowpea fields in Ghana, West Africa. Int. J. Biometeorol. 49, 106–112. https://doi.org/10.1007/s00484-004-0216-4.

Patrignani, A., Ochsner, T.E., 2015. Canopeo: a powerful new tool for measuring fractional Green canopy cover. Agron. J. 107, 2312–2320. https://doi.org/10.2134/agronj15.0150.

Pique, G., Carrer, D., Lugato, E., Fieuzal, R., Garisoain, R., Ceschia, E., 2023. About the assessment of cover crop albedo potential cooling effect: risk of the darkening feedback loop effects. Remote Sens. 15, 3231. https://doi.org/10.3390/rs15133231.

Post, D.F., Fimbres, A., Matthias, A.D., Sano, E.E., Accioly, L., Batchily, A.K., Ferreira, L. G., 2000. Predicting soil albedo from soil color and spectral reflectance data. Soil Sci. Soc. Am. J. 64, 1027–1034. https://doi.org/10.2136/sssaj2000.6431027x.

Powlson, D.S., Stirling, C.M., Thierfelder, C., White, R.P., Jat, M.L., 2016. Does conservation agriculture deliver climate change mitigation through soil carbon sequestration in tropical agro-ecosystems? Agric. Ecosyst. Environ. 220, 164–174. https://doi.org/10.1016/j.agee.2016.01.005.

R Core Team, 2023. _R: A Language and Environment for Statistical Computing_. R Foundation for Statistical Computing, Vienna, Austria. https://www.R-project.org.

Rosenberg, N.J., Blad, B.L., Verma, S.B., 1983. Microclimate: the Biological Environment. John Wiley & Sons.

Rost, J., Mayer, H., 2006. Comparative analysis of albedo and surface energy balance of a grassland site and an adjacent Scots pine forest. Clim. Res. 12.

Schwaiger, H.P., Bird, D.N., 2010. Integration of albedo effects caused by land use change into the climate balance: should we still account in greenhouse gas units? For. Ecol. Manag. 260, 278–286. https://doi.org/10.1016/j.foreco.2009.12.002.

Seneviratne, S.I., Phipps, S.J., Pitman, A.J., Hirsch, A.L., Davin, E.L., Donat, M.G., Hirschi, M., Lenton, A., Wilhelm, M., Kravitz, B., 2018. Land radiative management as contributor to regional-scale climate adaptation and mitigation. Nat. Geosci. 11, 88–96. https://doi.org/10.1038/s41561-017-0057-5.

Shumba, A., Chikowo, R., Corbeels, M., Six, J., Thierfelder, C., Cardinael, R., 2023. Long-term tillage, residue management and crop rotation impacts on N_2O and CH_4 emissions from two contrasting soils in sub-humid Zimbabwe. Agric. Ecosyst. Environ. 341, 108207. https://doi.org/10.1016/j.agee.2022.108207.

Shumba, A., Chikowo, R., Thierfelder, C., Corbeels, M., Six, J., Cardinael, R., 2024. Mulch application as the overarching factor explaining increase in soil organic carbon stocks under conservation agriculture in two 8-year-old experiments in Zimbabwe. SOIL 10, 151–165. https://doi.org/10.5194/soil-10-151-2024.

Sieber, P., Böhme, S., Ericsson, N., Hansson, P.-A., 2022. Albedo on cropland: Field-scale effects of current agricultural practices in Northern Europe. Agric. For. Meteorol. 321, 108978. https://doi.org/10.1016/j.agrformet.2022.108978.

Sieber, P., Ericsson, N., Hansson, P.-A., 2019. Climate impact of surface albedo change in life cycle assessment: implications of site and time dependence. Environ. Impact Assess. Rev. 77, 191–200. https://doi.org/10.1016/j.eiar.2019.04.003.

Smith, C.J., Kramer, R.J., Myhre, G., Alterskjær, K., Collins, W., Sima, A., Boucher, O., Dufresne, J.-L., Nabat, P., Michou, M., Yukimoto, S., Cole, J., Paynter, D., Shiogama, H., O'Connor, F.M., Robertson, E., Wiltshire, A., Andrews, T., Hannay, C., Miller, R., Nazarenko, L., Kirkevåg, A., Olivié, D., Fiedler, S., Lewinschal, A., Mackallah, C., Dix, M., Pincus, R., Forster, P.M., 2020. Effective radiative forcing and adjustments in CMIP6 models. Atmos. Chem. Phys. 20, 9591–9618. https://doi.org/10.5194/acp-20-9591-2020.

Thierfelder, C., Wall, P.C., 2009. Effects of conservation agriculture techniques on infiltration and soil water content in Zambia and Zimbabwe. Soil Tillage Res. 105, 217–227. https://doi.org/10.1016/j.still.2009.07.007.

Vogel, H., 1994. The Effect of Tillage on Topsoil Temperature and Strength in Coarse-grained Sands with Special Reference to a Tied Ridging System. Exp. Agric. 30 (1), 57–66. https://doi.org/10.1017/S001447970002384X.

Wang, S., Trishchenko, A.P., Sun, X., 2007. Simulation of canopy radiation transfer and surface albedo in the EALCO model. Clim. Dyn. 29, 615–632. https://doi.org/10.1007/s00382-007-0252-y.

Yan, G., Hu, R., Luo, J., Weiss, M., Jiang, H., Mu, X., Xie, D., Zhang, W., 2019. Review of indirect optical measurements of leaf area index: Recent advances, challenges, and perspectives. Agric. For. Meteorol. 265, 390–411. https://doi.org/10.1016/j.agrformet.2018.11.033.